Published on 19 September 2009. Downloaded by University of Michigan Library on 22/10/2014 13:10:09.

Four μ_4-oxo-bridged copper(II) complexes: magnetic properties and catalytic applications in liquid phase partial oxidation reactions†

Partha Roy,[a,b] Mahasweta Nandi,[c,d] Mario Manassero,[e] Mauro Riccó,[f] Marcello Mazzani,[f] Asim Bhaumik[c] and Pradyot Banerjee*[b]

Received 8th July 2009, Accepted 28th August 2009
First published as an Advance Article on the web 19th September 2009
DOI: 10.1039/b913556a

Four copper(II) complexes, $[Cu_4(O)(L^n)_2(CH_3COO)_4]$ with N_2O-donor Schiff-base ligands, where $\mathbf{HL^1}$ = 4-methyl-2,6-bis(cyclohexylmethyliminomethyl)phenol for complex **1**, $\mathbf{HL^2}$ = 4-methyl-2,6-bis(phenylmethyliminomethyl)phenol for complex **2**·CH_3CN, $\mathbf{HL^3}$ = 4-methyl-2,6-bis(((3-tri-fluoro-methyl)phenyl)methyliminomethyl)phenol for complex **3**, $\mathbf{HL^4}$ = 4-methyl-2,6-bis(((4-tri-fluoro-methyl)phenyl)methyliminomethyl)phenol for complex **4**, were synthesized and characterized by elemental analysis, FT-IR, UV-vis spectroscopy and finally by single crystal X-ray diffraction study. X-Ray analysis reveals that all of these are μ_4-oxo-bridged tetrameric copper(II) complexes. Four copper atoms arrange themselves around an oxygen atom tetrahedrally. Magnetic susceptibility measurements show the existence of very strong antiferromagnetic coupling among these ions ($J = -210.1$ to -271.3 cm^{-1}), mediated by the oxygen atoms. Catalysis of the epoxidation of cyclohexene, styrene, α-methylstyrene and *trans*-stilbene by these complexes has been carried out homogeneously as well as heterogeneously by immobilizing the metal complexes over 2D-hexagonal mesoporous silica. The results obtained in both the catalytic conditions show that the olefins are converted to the respective epoxides in good yield together with high selectivity.

Introduction

Multinuclear copper(II) complexes of Schiff-base ligands have been drawing special attention from researchers for a few decades because of their interesting properties as well as their applications in the fields of magnetism, catalysis, biology *etc.*[1–9] A dinucleating Schiff-base ligand, a condensate of 4-methyl-2,6-diformylphenol with 2-aminophenol, was reported by Robson for the first time in 1970.[10,11] Many examples of similar ligands of 4-methyl-2,6-diformylphenol have been reported.[12–16] Deprotonation of the phenolic –OH group and then bridging of two metal ions make them a potential dinucleating ligands. Hydroxo-, alkoxo-, and phenoxo-bridged dicopper(II) complexes involving a Cu_2O_2 bridging moiety with their relevance to copper enzymes are amply reported in the literature.[17–19] Schiff-base complexes with tetranuclear $\{Cu_4(\mu_4\text{-}O)\}$ cores are described in research articles and studied extensively.[14,20] The four copper atoms are arranged in a distorted tetrahedron keeping the μ_4-O at the center. The metals are also coordinated to phenoxide, halides or carboxylate groups to get extra stability. A considerable amount of research has been carried out to elucidate the magnetostructural relationship. Magnetic properties of Cu(II) ions in multinuclear metal–organic complexes are widely explored because copper(II) ions produce variable and distorted coordination geometries and have a simple electronic configuration.[21,22] There are many reports on the magnetic properties of multinuclear complexes with Cu(II). Ray and co-workers have reported μ_4-O-bridged Cu(II) complexes and studied their magnetic properties extensively. Temperature dependent magnetic studies reveal that there are antiferromagnetic interactions between the metal atoms.[23,24]

The transition metal complexes have been used as catalysts for the epoxidation of alkenes in the past few decades.[25,26] Epoxides are versatile synthetic compounds, constituting convenient building blocks for the synthesis of many products and fine chemicals.[27,28] A large number of publications concerns about the use of complexes of the transition metals Mn, Fe and Ni, primarily as highly enantioselective catalysts in the epoxidation of alkenes.[29–40] Several studies have focused on the preparation of the epoxides employing transition metal complexes as catalysts in the presence of several terminal oxidants such as NaOCl, peracid, *tert*-butyl hydroperoxide, hydrogen peroxide, molecular oxygen, *etc*. The reactions with hydrogen peroxide are attractive from the environmental view point[41] since water is produced as the only waste product when hydrogen peroxide is used as the oxidant. Catalytic reactions may be carried out either homogeneously or heterogeneously. The

---

[a] *Department of Chemistry, Jadavpur University, Jadavpur, Kolkata 700 032, India*
[b] *Department of Inorganic Chemistry, Indian Association for the Cultivation of Science, Jadavpur, Kolkata 700 032, India. E-mail: icpb@iacs.res.in; Fax: +91 33 2473-2805*
[c] *Department of Materials Science, Indian Association for the Cultivation of Science, Jadavpur, Kolkata 700 032, India*
[d] *Department of Integrated Science, Visva-Bharati University, Santiniketan, 731 235, India*
[e] *Dipartimento di Chimica Strutturale e Stereochimica Inorganica dell'Università di Milano, Via G. Venezian 21, 20133, Milano, Italy*
[f] *Dipartimento di Fisica, Università di Parma, Via G. Usberti, 7/a, 43100, Parma, Italy*

† Electronic supplementary information (ESI) available: A view of structures of complexes **2** and **3** (Fig. S1 and S2), temperature dependence of magnetization for complex **2**, **3** and **4** (Fig. S3, S4 and S5) and CIFs for four complexes. CCDC reference numbers 724021–724024. For ESI and crystallographic data in CIF or other electronic format see DOI: 10.1039/b913556a

Published on 19 September 2009. Downloaded by University of Michigan Library on 22/10/2014 13:10:09.

main problem in homogeneous catalysis is the separation of the catalyst, substrate, oxidant and product(s) because these are in a single phase with the solvent. Poor recycling efficiencies of the catalysts are also noted in the case of homogeneous catalysis. A catalyst with high recycling capacity would require minimum effort for its separation and seems to be the most desirable one in an industrial process. For this reason, attention has been prompted on the use of heterogeneous catalysts for over the last few decades.[42–44] The heterogenization of transition metal-based catalysts on different solid supports, *e.g.* silica,[45,46] polymers,[47] mesoporous materials,[48–50] activated carbons,[51,52] pillared clays,[53] and zeolites,[54] has been made effectively. The immobilization and application of copper(II) complexes in heterogeneous catalysis have not been extensively explored.[55] Recently our group has reported the synthesis and characterization of some Schiff-base complexes of Ni(II)[56] and Cu(II),[57] and explored their catalytic activity towards the oxidation of alkenes. The complexes immobilized on mesoporous silica acted as efficient catalysts for the catalytic reaction to yield epoxides as the major products.

We report here the synthesis, characterization, magnetic and catalytic properties of four copper(II) complexes $[Cu_4(O)(\mathbf{L}^n)_2(CH_3COO)_4]$ with N_2O-donor Schiff-base ligands, where $\mathbf{HL}^1$ = 4-methyl-2,6-bis(cyclohexylmethyliminomethyl)phenol for complex **1**, $\mathbf{HL}^2$ = 4-methyl-2,6-bis(phenylmethyliminomethyl)phenol for complex $\mathbf{2}\cdot CH_3CN$, $\mathbf{HL}^3$ = 4-methyl-2,6-bis(((3-tri-fluoromethyl)phenyl)methyliminomethyl)phenol for complex **3**, $\mathbf{HL}^4$ = 4-methyl-2,6-bis(((4-tri-fluoromethyl)phenyl)methyliminomethyl)phenol for complex **4**. Single crystal X-ray analysis has revealed that all complexes have similar structures. Homogeneous catalytic reactions for the epoxidation of cyclohexene, styrene, α-methylstyrene and *trans*-stilbene are carried out using hydrogen peroxide as the oxidant in presence of the complexes as catalysts. The complexes **1–4** have been found to be highly active catalysts. The catalytic conversion could be achieved heterogeneously. The heterogeneous catalysts have been prepared by immobilizing the complexes on 2D-hexagonal mesoporous silica. The immobilized catalyst is employed for the epoxidation of cyclohexene, styrene, α-methylstyrene and *trans*-stilbene using hydrogen peroxide as the oxidant. The results show that the conversion of the alkene occurs with high yield and high selectivity towards the corresponding epoxide.

Experimental

Materials and physical methods

Cyclohexylmethylamine, 1-phenylmethanamine, 3-trifluoromethyl-1-phenylmethanamine, 4-trifluoromethyl-1-phenylmethanamine, cyclohexene, styrene, α-methylstyrene, *trans*-stilbene, cycloheptanone, copper(II) acetate monohydrate, tetramethylammonium hydroxide (TMAOH) and tetraethyl orthosilicate (TEOS) were purchased from Aldrich and used without purification. Other reagents were purchased from commercial sources and used without further purification. 4-Methyl-2,6-diformylphenol was synthesized following a published procedure.[58] Solvents used for spectroscopic studies were purified and dried by standard procedures before use.[59] Elemental analysis was carried out in a 2400 Series-II CHN analyzer, Perkin Elmer, USA. FT-IR spectra were obtained on a Nicolet MAGNA-IR 750 spectrometer with samples prepared as KBr pellets. The ESI-MS was recorded on Qtof Micro YA263 mass spectrometer. Magnetic measurements were performed using a Quantum Design MPMS XL SQUID magnetometer, capable of a field as high as 5 T, working in the temperature range 5–300 K. Characterization of the samples by powder X-Ray diffraction was performed by using a Bruker AXS D8 Advanced SWAX diffractometer, where the small and wide-angle goniometers are mounted. The X-ray source was Cu-Kα radiation (α = 0.15406 nm) with an applied voltage and current of 40 kV and 20 mA, respectively. Mesophases of different samples were analyzed using a JEOL, JEM 2010 transmission electron microscope at an accelerating voltage of 200 kV. N_2 adsorption measurements were carried out using a Bel Japan Inc. Belsorp-HP surface area analyzer at 77 K. Pre-treatment of the samples was done at 473 K for 3 h under high vacuum. A Shimadzu AA-6300 double beam atomic absorption spectrophotometer (AAS) was used for determining the percentage loading of Cu through wet chemical analysis. Absorption spectra were studied on a Shimadzu UV 2100 spectrophotometer. UV-visible diffuse reflectance spectra (DRS) for the immobilized catalysts were recorded on a Shimadzu 2401PC UV-visible spectrophotometer with an integrating sphere attachment using $BaSO_4$ as the background standard. Gas chromatography analysis was performed with an Agilent Technologies 6890 N network GC system equipped with a fused silica capillary column (30 m × 0.32 mm) and a FID detector. All experiments were carried out in air and room temperature unless reported otherwise.

The Schiff-base ligands, 4-methyl-2,6-bis(cyclohexylmethyliminomethyl)phenol ($\mathbf{HL}^1$)[16] and 4-methyl-2,6-bis(phenylmethyliminomethyl)phenol ($\mathbf{HL}^2$),[60,61] were synthesized following the published procedures.

Synthesis of 4-methyl-2,6-bis(((3-tri-fluoromethyl)phenyl)methyliminomethyl)phenol ($\mathbf{HL}^3$) and 4-methyl-2,6-bis(((4-tri-fluoromethyl)phenyl)methyliminomethyl)phenol ($\mathbf{HL}^4$)

These two ligands were prepared following the same procedure with a slight modification.[60] To a solution of 4-methyl-2,6-diformylphenol (0.656 g, 4 mmol) in 15 mL of acetonitrile was added the respective amine (0.857 g, 8 mmol) (3-trifluoromethyl-1-phenylmethanamine for $\mathbf{HL}^3$ and 4-trifluoromethyl-1-phenylmethanamine for $\mathbf{HL}^4$) in 10 mL acetonitrile. The reaction mixture was refluxed for 3 h. The solution was filtered, concentrated on a rotary evaporator to dryness and kept overnight at 4 °C. The resulting Schiff base is solid and it has been recrystallized from acetonitrile.

Data for $\mathbf{HL}^3$. Yield = 1.68 g, 88%. Found: C, 62.70; H, 4.16; N, 5.90%; $C_{25}H_{20}N_2OF_6$ requires C, 62.76; H, 4.21; N, 5.86%; FT-IR (KBr phase) ν_{max}/cm^{-1}: 2921 (CH), 1639 (CN); δ_H (300 MHz, $CDCl_3$, Me_4Si) 2.32 (3H, s, Ar-CH_3), 4.86 (4H, s, CH), 7.32–7.52 (10H, m, Ar-CH), 8.70 (2H, s, HC=N). *m*/*z* (ESI) 479.4370 ($C_{25}H_{21}N_2OF_6^+$ requires 479.4375).

Data for $\mathbf{HL}^4$. Yield = 1.72 g, 90%. Found: C, 62.71; H, 4.15; N, 5.82%; $C_{25}H_{20}N_2OF_6$ requires C, 62.76; H, 4.21; N, 5.86.%; FT-IR (KBr phase) ν_{max}/cm^{-1}: 2896 (CH), 1643 (CN); δ_H (300 MHz, $CDCl_3$, Me_4Si) 2.31 (3H, s, Ar-CH_3), 4.87 (4H, s, CH), 7.36–7.62 (10H, m, Ar-CH), 8.69 (2H, s, HC=N). *m*/*z* (ESI) 479.4371 ($C_{25}H_{21}N_2OF_6^+$ requires 479.4375).

This journal is © The Royal Society of Chemistry 2009

View Article Online

Published on 19 September 2009. Downloaded by University of Michigan Library on 22/10/2014 13:10:09.

Table 1 Crystal data for complex **1**, **2**·CH_3CN, **3** and **4**

Complex	**1**	**2**·CH_3CN	**3**	**4**
Empirical formula	$C_{54}H_{78}Cu_4N_4O_{11}$	$C_{56}H_{57}Cu_4N_5O_{11}$	$C_{58}H_{50}Cu_4F_{12}N_4O_{11}$	$C_{58}H_{50}Cu_4F_{12}N_4O_{11}$
Formula weight	1213.40	1230.27	1461.21	1461.21
Crystal system	Tetragonal	Triclinic	Triclinic	Triclinic
Space group	$I4_1/a$	$P\bar{1}$	$P\bar{1}$	$P\bar{1}$
Color	Green	Green	Green	Green
a/Å	13.2184(7)	12.6557(7)	12.5687(7)	12.4065(7)
b/Å	13.2184	14.5524(8)	15.4115(9)	15.4152(8)
c/Å	34.169(2)	15.7123(9)	17.0077(10)	16.9396(9)
α (°)	90	109.029(1)	111.009(1)	99.450(2)
β (°)	90	91.840(1)	96.640(1)	91.150(2)
γ (°)	90	92.010(1)	95.800(1)	93.010(2)
V/Å^3	5970.2(6)	2731.0(16)	3018.5(3)	3190.0(3)
Z	4	2	2	2
D_{calc} (g cm^{-3})	1.350	1.496	1.608	1.521
Crystal dimensions/mm	0.15 × 0.15 × 0.30	0.10 × 0.50 × 0.50	0.15 × 0.25 × 0.45	0.24 × 0.30 × 0.45
μ(Mo-Kα)/mm^{-1}	1.465	1.603	1.490	1.410
Min. and max. transmission factors	0.857, 1.000	0.748, 1.000	0.833, 1.000	0.876, 1.000
F(000)	2536	1264	1476	1476
T/K	296	150	296	296
λ(Mo-Kα)	0.71073	0.71073	0.71073	0.71073
Max. and min. θ/°	30.00, 3.00	28.00, 3.00	28.00, 3.00	29.00, 3.00
Total data, unique data	47 777, 4866	50 607, 13 996	36 534, 14 676	61 577, 22 297
R_{int}	0.0410	0.0226	0.0314	0.0402
Reciprocal space explored	Full sphere	Full sphere	Full sphere	Full sphere
Final R_2 and R_{2w} indices[a] (F^2, all reflections)	0.064, 0.093	0.047, 0.080	0.078, 0.117	0.106, 0.145
Conventional R_1 index ($I > 2\sigma(I)$)	0.035	0.028	0.048	0.051
Reflections with ($I > 2\sigma(I)$)	2575	11 002	7998	8481
No. of variables	190	685	802	802
Goodness-of-fit[b]	0.979	1.069	1.070	0.961

[a] $R_2 = [\sum(|F_o^2 - kF_c^2|/\sum F_o^2]$, $R_{2w} = [\sum w(F_o^2 - kF_c^2)^2/\sum w(F_o^2)^2]^{1/2}$. [b] $[\sum w(F_o^2 - kF_c^2)^2/(N_o - N_v)]^{1/2}$, where $w = 4F_o^2/\sigma(F_o^2)^2$, $\sigma(F_o^2) = [\sigma^2(F_o^2) + (0.04F_o^2)^2]^{1/2}$, N_o is the number of observations, and N_v the number of variables.

Syntheses of complexes 1, 2·CH_3CN, 3 and 4

Complexes **1**, **2**·CH_3CN, **3** and **4** were synthesized using a common procedure. Typically, to an acetonitrile solution (10 mL) of ligand (0.3 mmol), 0.106 g for **HL**^{1}, 0.102 g for **HL**^{2}, 0.144 g for **HL**^{3} and 0.144 g for **HL**^{4}) was added copper(II) acetate monohydrate (0.6 mmol, 0.120 g). The mixture was stirred for 45 min. The color of the mixture was green which was refluxed for 1 h. It was cooled and filtered. The filtrate was kept at ambient temperature. Green single crystals suitable for X-ray diffraction study were produced within a few days.

Data for **1**. Yield = 0.36 g, 70%. Found: C, 53.38; H, 6.44; N, 4.57%; $C_{54}H_{78}Cu_4N_4O_{11}$ requires C, 53.45; H, 6.48; N, 4.62%.

Data for **2**·CH_3CN. Yield = 0.24 g, 65%. Found: C, 54.58; H, 6.64; N, 4.57%; $C_{56}H_{57}Cu_4N_5O_{11}$ requires C, 54.68; H, 4.67; N, 4.55%.

Data for **3**. Yield = 0.32 g, 72%. Found: C, 47.61; H, 3.43; N, 3.88%; $C_{58}H_{50}Cu_4F_{12}N_4O_{11}$ requires C, 47.68; H, 3.45; N, 3.83%.

Data for **4**. Yield = 0.33 g, 75%. Found: C, 47.63; H, 3.40; N, 3.88%; $C_{58}H_{50}Cu_4F_{12}N_4O_{11}$ requires C, 47.68; H, 3.45; N, 3.83%.

X-Ray data collections and structure determinations

Crystal data of complexes **1**, **2**·CH_3CN, **3** and **4** are summarized in Table 1. The diffraction experiments were carried out on a Bruker SMART CCD area-detector diffractometer at 296 K for complexes **1**, **3** and **4**, 150 K for **2**·CH_3CN. No crystal decay was observed, so that no time-decay correction was needed. The collected frames were processed with the software SAINT,[62] and an empirical absorption correction was applied (SADABS[63]) to the collected reflections. The calculations were performed using the Personal Structure Determination Package[64] and the physical constants tabulated therein.[65] The structures were solved by direct methods (SHELXS[66]) and refined by full-matrix least-squares using all reflections and minimising the function $\sum w(F_o^2 - kF_c^2)^2$ (refinement on F^2). In compound **1** the three toluylic hydrogen atoms (which are disordered by crystallographic symmetry) bonded to atom C5 were not detected in the final Fourier maps and were ignored. Again in compound **1**, the hydrogen atom H15, bonded to C6, and the three methylic hydrogen atoms of the acetato ligand, were detected in the final Fourier maps and included in the structure factor calculations, but not refined. In compounds, **2**·CH_3CN, **3**, and **4**, all the hydrogen atoms of the CH_3 groups either toluylic or belonging to an acetato ligand or to CH_3CN, were detected in the final Fourier maps, and included in the structure factor calculations, but not refined. All the other hydrogen atoms of four complexes were placed in their ideal positions (C–H = 0.97 Å), with the thermal parameter U being 1.10 times that of the atom to which they are attached, and included in the structure factor calculations, but not refined. All the non-hydrogen atoms of the four complexes were refined with anisotropic thermal parameters. In the final Fourier maps the maximum residuals were 0.98(23) e Å^{-3} at 0.08 Å from Cu1, 0.49(12) e Å^{-3} at 0.85 Å from Cu1, 1.33(27) e Å^{-3} at 1.13 Å from O10, and 1.44(54) e Å^{-3} at 0.53 Å from Cu4, in compounds **1**, **2**·CH_3CN, **3**, and **4**, respectively. Minimum peaks (holes) in the

Published on 19 September 2009. Downloaded by University of Michigan Library on 22/10/2014 13:10:09.

final Fourier maps of the four compounds, in the same order, were −0.42(23) e Å^{-3}, −0.45(12) e Å^{-3}, −1.04(27) e Å^{-3}, and −0.83(54) e Å^{-3}, respectively.

CCDC 724021, 724022, 724023 and 724024 contain the supplementary crystallographic data of complexes **1**, **2**·CH_3CN, **3** and **4**, respectively. For crystallographic data in CIF or other electronic format see DOI: 10.1039/b913556a.

Preparation of the immobilized catalysts

Highly ordered 2D-hexagonal mesoporous silica was synthesized using a cationic (cetyltrimethylammonium bromide, CTAB) and non-ionic (Brij 35, $C_{12}H_{25}$–$(OC_2H_4)_{23}$–OH, a polyether and aliphatic hydrocarbon chain surfactant) mixed surfactant system as the self-assembled structure directing agent (SDA) in the presence of tartaric acid (TA) as a mineralizer. Tetraethyl orthosilicate (TEOS) was used as the silica source. In a typical synthesis, 4.44 g CTAB and 2.5 g Brij 35 were dissolved in an acidic aqueous solution of TA (1.17 g in 60.0 g of H_2O) under vigorous stirring at room temperature for 1 h. This was followed by the addition of 7.0 g TEOS under continuous stirring. After 2 h of continuous stirring, tetramethylammonium hydroxide (TMAOH, 25% aqueous) was added dropwise and the pH was maintained at *ca.* 11.2. The resulting mixture was aged overnight under stirring at room temperature and then treated hydrothermally at 353 K for 72 h without stirring. The solid product was collected by filtration, washed several times with water and dried under vacuum at room temperature. The resulting powder was calcined in the flow of air at 723 K for 8 h to remove all the organic surfactants.

Immobilization of the metal complexes was carried out by dispersing 0.5 g of the mesoporous silica in a solution containing 0.1 g of the metal complex dissolved in 25 ml of dry acetonitrile, followed by vigorous stirring at room temperature for 4 h. Then the solid was filtered, washed with acetonitrile and dried under vacuum.

Heterogeneous catalysis

For the heterogeneous oxidation of olefin, the reactions were performed in a magnetically stirred two necked round-bottomed flask fitted with a condenser and placed in a temperature-controlled oil bath. Typically, 0.5 g of the substrate was taken in 5 ml acetonitrile (solvent), followed by the addition of 0.1 g of the immobilized catalyst and the mixture was then preheated to 333 K. The reaction was started with the addition of hydrogen peroxide (equimolar with respect to the substrate). Aliquots from reaction mixtures were collected at regular intervals. After cooling, cycloheptanone was added as the internal standard. The substrate and product(s) from the reaction mixture were analyzed by gas chromatography. They were identified by the comparison with known standards.

Homogeneous catalysis

The homogeneous catalysis was carried out at 298 K by a process similar to that adopted for heterogeneous catalysis. Typically, 0.5 g of the substrate was taken in a magnetically stirred two necked round-bottomed flask fitted with a condenser in 5 ml acetonitrile, followed by the addition of 0.01 mmol of the complex at room temperature. The reaction was started with the addition of hydrogen peroxide (equimolar with respect to the substrate). Aliquots from reaction mixtures were collected at regular intervals. After cooling, cycloheptanone as the internal standard and 10 ml of diethyl ether for extracting the reactants and products were added. The substrate and product(s) from the reaction mixture were analyzed by gas chromatography. They were identified by the comparison with known standards.

A blank experiment for the epoxidation of cyclohexene, as the representative case, was carried out homogeneously and heterogeneously without addition of any catalyst under the same experimental conditions.

Results and discussion

Synthesis and IR spectra

The ligands have been prepared by simple Schiff-base condensation between one equivalent of 4-methyl-2,6-diformylphenol and two equivalent of the respective amine in acetonitrile. The complexes have been synthesized by the reaction between the ligand and copper(II) acetate monohydrate in acetonitrile. Acetate ion from copper(II) acetate may deprotonate the phenolic proton of ligand. The acetate moieties are coordinated to the metal atom to give added stability to the complex.

FT-IR spectra of both the ligands and complexes were obtained with samples prepared as KBr pellets. FT-IR spectra of the ligands show a number of strong ν_{C-H} bands at 2800–3000 cm^{-1}. The complexes also show strong ν_{C-H} bands in this range.[67,68] **HL^1**, **HL^2**, **HL^3** and **HL^4** show strong bands at 1637, 1635, 1639 and 1643 cm^{-1} respectively, and these bands may be assigned to the C=N bond. The complexes **1**, **2**·CH_3CN, **3** and **4** show IR bands at 1629, 1625, 1630 and 1632 cm^{-1} respectively confirming the retention of C=N bond in the complex. The complexes show a sharp band of medium intensity at around 560 to 570 cm^{-1} for the characteristic T_2 mode of the Cu_4O core.[69] The spectra of the ligands miss these bands as expected.

Description of crystal structures of complexes

Complex **1** crystallizes in the tetragonal space group $I4_1/a$ from acetonitrile. A perspective view of the molecule is shown in Fig. 1. Selected bond lengths and bond angles are listed in Table 2. The molecule has crystallographic site symmetry 4-. It is a discrete tetrametallic monomer, with only one copper atom in the asymmetric unit. Atom O1 lies in a site having crystallographic symmetry 4-, and is bonded to four copper atoms in a slightly distorted tetrahedral arrangement. The Cu atom is coordinated to a μ_4-oxido oxygen atom O1, one μ_2-phenoxido oxygen atom O2 and one nitrogen atom N1 of the dinucleating ligand, 4-methyl-2,6-bis(cyclohexylmethyliminomethyl)-phenolate (**L^{1-}**), and two acetato oxygen atoms O3 and O4 from two different acetato

Table 2 Selected bond lengths (Å) and bond angles (°) of complex **1**

Cu–O1	1.919(1)	Cu–O2	1.975(1)
Cu–O3	1.942(1)	Cu–N1	1.979(2)
O1–Cu–O2	78.4(1)	O1–Cu–O3	94.8(1)
O1–Cu–N1	164.0(1)	O2–Cu–O3	172.1(1)
O2–Cu–N1	90.9(1)	O3–Cu–N1	96.6(1)

View Article Online

Published on 19 September 2009. Downloaded by University of Michigan Library on 22/10/2014 13:10:09.

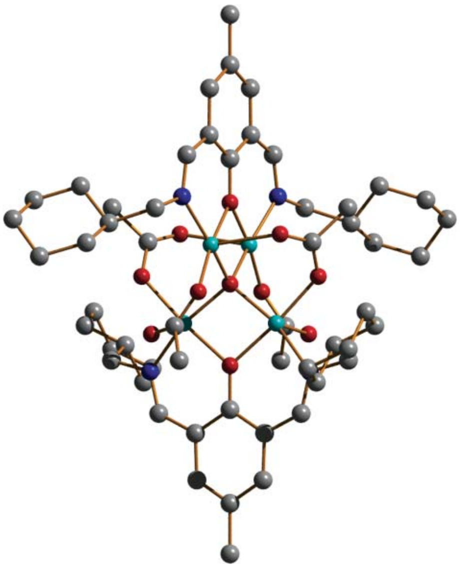

Fig. 1 A perspective view of complex **1**. Hydrogen atoms omitted for clarity.

moieties. The copper atom is in a distorted square pyramidal geometry as revealed by the trigonal index, τ, which is found to be 0.135. The value of τ is defined as the difference between the two largest donor–metal–donor angles divided by 60, a value which is 0 for the ideal square pyramid and 1 for the trigonal bipyramid.[70] The O1, O2, N1 and O3 atoms form the basal plane of the square pyramid, whereas O4 occupies the apical position. The Cu–O4 bond length is quite long compared to the other Cu–donor bond distances. The Cu–donor bond lengths are in good agreement with reported values.[8,9,14]

Complexes **2**·CH_3CN, **3** and **4** crystallize in the same space group, triclinic ($P\bar{1}$). Perspective views of the complexes are shown in the ESI† (Fig. S1, S2) and Fig. 2, respectively. Selected bond lengths and bond angles of complexes **2**·CH_3CN, **3** and **4** are given in Table 3, 4 and 5, respectively. Copper and donor atom connectivities are the same for all the complexes, so descriptions of the crystal structures of the three

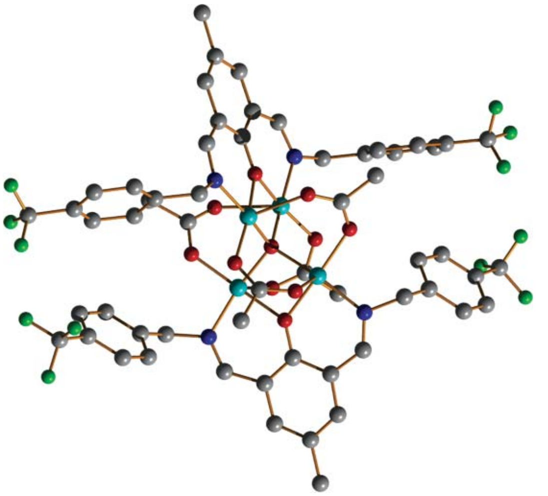

Fig. 2 A perspective view of complex **4**. Hydrogen atoms were omitted for clarity.

Table 3 Selected bond lengths (Å) and bond angles (°) of complex **2**·CH_3CN

Cu1–O1	1.937(1)	Cu3–O1	1.924(1)
Cu1–O2	1.983(1)	Cu3–O3	1.987(1)
Cu1–O4	1.917(1)	Cu3–O5	2.221(1)
Cu1–O6	2.274(1)	Cu3–O7	1.926(1)
Cu1–N1	2.000(2)	Cu3–N3	1.998(2)
Cu2–O1	1.910(1)	Cu4–O1	1.920(1)
Cu2–O2	1.974(1)	Cu4–O3	1.968(1)
Cu2–O10	1.932(1)	Cu4–O9	1.927(1)
Cu2–N2	1.976(1)	Cu4–N4	1.963(1)
O1–Cu1–O2	79.9(1)	O1–Cu3–N3	164.2(1)
O1–Cu1–O4	96.5(1)	O3–Cu3–O5	90.7(1)
O1–Cu1–O6	92.2(1)	O3–Cu3–O7	166.2(1)
O1–Cu1–N1	163.5(1)	O3–Cu3–N3	89.6(1)
O2–Cu1–O4	170.1(1)	O5–Cu3–O7	102.8(1)
O2–Cu1–O6	86.3(1)	O5–Cu3–N3	92.0(1)
O2–Cu1–N1	90.0(1)	O7–Cu3–N3	92.2(1)
O4–Cu1–O6	103.1(1)	O1–Cu4–O3	80.3(1)
O4–Cu1–N1	91.2(1)	O1–Cu4–O9	93.2(1)
O6–Cu1–N1	100.3(1)	O1–Cu4–N4	170.9(1)
O1–Cu2–O2	80.8(1)	O3–Cu4–O9	161.8(1)
O1–Cu2–O10	94.6(1)	O3–Cu4–N4	91.4(1)
O1–Cu2–N2	168.5(1)	O9–Cu4–N4	93.5(1)
O2–Cu2–O10	168.4(1)	Cu1–O1–Cu2	101.4(1)
O2–Cu2–N2	89.5(1)	Cu1–O1–Cu3	111.9(1)
O10–Cu2–N2	93.8(1)	Cu1–O1–Cu4	114.3(1)
O1–Cu3–O3	79.8(1)	Cu2–O1–Cu3	119.7(1)
O1–Cu3–O5	99.7(1)	Cu2–O1–Cu4	108.2(1)
O1–Cu3–O7	95.5(1)	Cu3–O1–Cu4	101.8(1)

Table 4 Selected bond lengths (Å) and bond angles (°) of complex **3**

Cu1–O1	1.910(2)	Cu3–O1	1.918(2)
Cu1–O2	1.990(2)	Cu3–O3	1.969(2)
Cu1–O4	2.328(2)	Cu3–O5	1.941(2)
Cu1–O6	1.943(2)	Cu3–O7	2.340(3)
Cu1–N1	1.974(3)	Cu3–N3	2.000(3)
Cu2–O1	1.924(2)	Cu4–O1	1.919(2)
Cu2–O2	1.984(3)	Cu4–O3	1.973(2)
Cu2–O8	1.924(3)	Cu4–O9	2.427(3)
Cu2–O10	2.288(3)	Cu4–O11	1.960(3)
Cu2–N2	1.983(2)	Cu4–N4	1.971(2)
O1–Cu1–O2	79.2(1)	O1–Cu3–N3	161.3(1)
O1–Cu1–O4	95.6(1)	O3–Cu3–O5	172.6(1)
O1–Cu1–O6	95.0(1)	O3–Cu3–O7	84.6(1)
O1–Cu1–N1	169.4(1)	O3–Cu3–N3	90.4(1)
O2–Cu1–O4	87.8(1)	O5–Cu3–O7	100.8(1)
O2–Cu1–O6	166.3(1)	O5–Cu3–N3	94.0(1)
O2–Cu1–N1	91.0(1)	O7–Cu3–N3	96.7(1)
O4–Cu1–O6	105.2(1)	O1–Cu4–O3	79.0(1)
O4–Cu1–N1	87.7(1)	O1–Cu4–O9	90.0(1)
O6–Cu1–N1	93.8(1)	O1–Cu4–O11	93.6(1)
O1–Cu2–O2	79.0(1)	O1–Cu4–N4	165.1(1)
O1–Cu2–O8	93.8(1)	O3–Cu4–O9	80.5(1)
O1–Cu2–O10	96.0(1)	O3–Cu4–O11	163.8(1)
O1–Cu2–N2	168.3(1)	O3–Cu4–N4	90.6(1)
O2–Cu2–O8	162.3(1)	O9–Cu4–O11	114.2(1)
O2–Cu2–O10	87.5(1)	O9–Cu4–N4	98.9(1)
O2–Cu2–N2	90.8(1)	O11–Cu4–N4	93.6(1)
O8–Cu2–O10	109.5(1)	Cu1–O1–Cu2	103.4(1)
O8–Cu2–N2	94.4(1)	Cu1–O1–Cu3	111.2(1)
O10–Cu2–N2	89.1(1)	Cu1–O1–Cu4	111.3(1)
O1–Cu3–O3	79.2(1)	Cu2–O1–Cu3	119.6(1)
O1–Cu3–O5	95.0(1)	Cu2–O1–Cu4	108.7(1)
O1–Cu3–O7	97.7(1)	Cu3–O1–Cu4	102.8(1)

View Article Online

Published on 19 September 2009. Downloaded by University of Michigan Library on 22/10/2014 13:10:09.

Table 5 Selected bond lengths (Å) and bond angles (°) of complex **4**

Cu1–O1	1.910(2)	Cu3–O1	1.915(2)
Cu1–O2	1.980(2)	Cu3–O3	1.979(2)
Cu1–O6	1.927(2)	Cu3–O5	1.929(2)
Cu1–N1	1.979(3)	Cu3–N3	1.989(3)
Cu2–O1	1.923(2)	Cu4–O1	1.925(2)
Cu2–O2	1.983(2)	Cu4–O3	1.977(2)
Cu2–O8	1.942(2)	Cu4–O9	2.271(2)
Cu2–O10	2.261(3)	Cu4–O11	1.929(3)
Cu2–N2	1.982(2)	Cu4–N4	1.995(2)
O1–Cu1–O2	80.1(1)	O1–Cu3–O3	79.7(1)
O1–Cu1–O6	93.4(1)	O1–Cu3–O5	94.6(1)
O1–Cu1–N1	169.0(1)	O1–Cu3–N3	166.9(1)
O2–Cu1–O6	164.7(1)	O3–Cu3–O5	167.2(1)
O2–Cu1–N1	90.6(1)	O3–Cu3–N3	90.5(1)
O6–Cu1–N1	94.2(1)	O5–Cu3–N3	93.1(1)
O1–Cu2–O2	79.7(1)	O1–Cu4–O3	79.5(1)
O1–Cu2–O8	95.4(1)	O1–Cu4–O9	95.8(1)
O1–Cu2–O10	97.2(1)	O1–Cu4–O11	94.7(1)
O1–Cu2–N2	164.5(1)	O1–Cu4–N4	164.5(1)
O2–Cu2–O8	170.0(1)	O3–Cu4–O9	85.3(1)
O2–Cu2–O10	89.3(1)	O3–Cu4–O11	168.1(1)
O2 Cu2 N2	89.9(1)	O3–Cu4–N4	90.3(1)
O8 Cu2 O10	99.9(1)	O9–Cu4–O11	105.8(1)
O8 Cu2 N2	93.1(1)	O9–Cu4–N4	95.0(1)
O10 Cu2 N2	94.1(1)	O11–Cu4–N4	93.0(1)
Cu1 O1 Cu2	102.4(1)	Cu1–O1–Cu3	109.9(1)
Cu1 O1 Cu4	116.1(1)	Cu2–O1–Cu3	115.8(1)
Cu2 O1 Cu4	110.8(1)	Cu3–O1–Cu4	102.4(1)

complexes are made in a general manner. The metal and donor connectivities are shown in Scheme 1. These are discrete tetranuclear complexes. The asymmetric unit consists of four copper atoms, two N_2O-donor dinucleating ligands, 4-methyl-2,6-bis(phenylmethyliminomethyl)phenolate ($\mathbf{L^{2-}}$) for complex **2**·CH_3CN, 4-methyl-2,6-bis(((3-tri-fluoromethyl)phenyl)methyliminomethyl)phenolate ($\mathbf{L^{3-}}$) for complex **3** and 4-methyl-2,6-bis(((4-tri-fluoromethyl)phenyl)methyliminomethyl)phenolate ($\mathbf{L^{4-}}$) for complex **4**, one μ_4-oxido and four acetato ions. Cu1 is bonded to one μ_4-oxido oxygen atom O1, one μ_2-phenoxido oxygen atom O2 and one nitrogen atom N1 of the same dinucleating ligand, and two oxygen atoms O4 and O6 from two different acetato ions. The Cu1 atom is in a distorted square pyramidal geometry as revealed by the trigonal index value listed in Table 6. Cu1–O_{apical} bond lengths are long compared to other Cu1–donor bond distances. The Cu2 atom is linked to one oxygen atom O1, one μ_2-phenoxido oxygen atom O2 and one nitrogen atom N2 of the same dinucleating ligand, and two oxygen atoms O8 and O10 from two different acetato ions. This copper atom is also in a distorted square pyramidal geometry (Table 6). The Cu3 atom is attached to one oxygen atom O1, one μ_2-phenoxido oxygen atom O3 and one nitrogen atom N3 of the dinucleating ligand, two oxygen atoms O5 and O7 from two different acetato ions. These donor atoms make a square pyramidal environment around Cu3. Here all the Cu1–O_{apical} bond lengths are longer compared to other Cu1–donor bond length values. The Cu4 atom is coordinated to the μ_4-oxido oxygen atom O1, one μ_2-phenoxido oxygen atom O3 and one nitrogen atom N4 of the dinucleating ligand, and two oxygen atoms O9 and O11 from two different acetato ions. This atom is also in a distorted square pyramidal geometry. Cu1–donor bond lengths are in good agreement with the reported one.[8,9,14]

Table 6 Trigonal index values of the complexes **2**·CH_3CN, **3** and **4**

Complex	Cu1	Cu2	Cu3	Cu4
2·CH_3CN	0.110	0.002	0.033	0.152
3	0.052	0.100	0.188	0.022
4	0.072	0.092	0.005	0.045

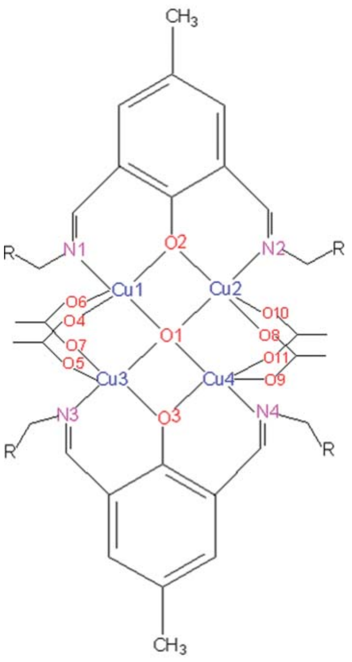

Scheme 1 R = phenyl for complex **2**·CH_3CN, (3-trifluoromethyl)phenyl for complex **3** and (4-trifluoromethyl)phenyl for complex **4**.

Magnetic properties of the complexes

DC SQUID magnetometry, performed on powder samples, gave similar results in all of the complexes. A representative curve, recorded for complex **1**, displaying the temperature dependence of magnetization is shown in Fig. 3. Similar plots for the temperature

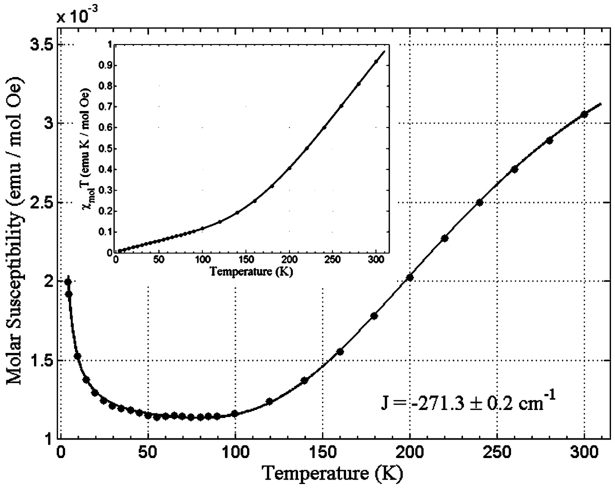

Fig. 3 Temperature dependence of magnetization for complex **1**, measured in a magnetic field of 1 kOe. A strong antiferromagnetic coupling, persistent up to 325 K, characterizes the (Cu_4–O) cluster.

This journal is © The Royal Society of Chemistry 2009

Published on 19 September 2009. Downloaded by University of Michigan Library on 22/10/2014 13:10:09.

dependence of magnetization of complexes **2–4** are given in the ESI† (Fig. S3, S4 and S5). The oxygen-mediated exchange interaction between Cu ions is known to be relatively strong and of antiferromagnetic type. Thus the magnetic behavior of the (Cu_4–O) cluster, taking into account its symmetry point group, can be properly described by an Heisenberg Hamiltonian including three different coupling constants. Unfortunately the resulting expression for the antiferromagnetic susceptibility[18,71,72] is not suitable for least square analysis of the data, as the three coupling constants highly correlate. An approximate isotropic model shall then be introduced: in the regime of strong antiferromagnetic (AFM) coupling, only the ground state $S = 0$ and the first excited state $S = 1$ are accessible at temperatures up to 300 K. Consequently the Bleaney–Bowers formula,[73] valid for a two-state magnetic system, can be adopted. The model function for least-square analysis is then written as:

$$\chi(T) = 6\frac{C}{T}\frac{\exp\left(\dfrac{2J}{k_B T}\right)}{1+3\exp\left(\dfrac{2J}{k_B T}\right)} + \frac{3}{4}\frac{\rho C}{T - T_c} + \chi_0.$$

Apart from the major AFM contribution, it includes a Curie–Weiss component, related to a small fraction ρ of paramagnetic impurities (typically 1%, except for complex **3** which contains a much higher paramagnetic impurities concentration, 27.5%), and a temperature-independent susceptibility χ_0, which accounts for ferromagnetic impurities, the quartz sample holder contribution and possible Van Vleck paramagnetism.

The estimated values of the antiferromagnetic coupling constant are $J = -210.1 \pm 0.1$ cm^{-1} for complex **4**, $J = -219.9 \pm 0.2$ cm^{-1} for **2**, $J = -227.2 \pm 0.1$ cm^{-1} for complex **3**, $J = -271.3 \pm 0.2$ cm^{-1} for complex **1**. These values are in good agreement with data previously reported for similar systems[18,72] and their distribution is likely to be due to distortions induced in the cluster geometry by the different ligands which characterize each complex.

The amplitude of the signal, which for complex **1** is $C = -1.60 \pm 0.01$ emu K mol^{-1} Oe^{-1}, corresponds to slightly less than the expected value of 4 μ_B per formula unit. Such a reduction is likely to be due to a small magnetic anisotropy term, suggested by the cluster structure, which was not taken into account in the calculations as its inclusion would largely increase the complexity of the susceptibility calculations.[74]

Powder X-ray diffraction and nitrogen sorption studies

Low angle X-ray diffraction patterns of the mesoporous host as well as the one of the representative immobilized complex **1** (**IC-1**) are shown in Fig. 4. All four peaks for 100, 110, 200 and 210 planes of the 2D hexagonal mesophase[75] were observed for the calcined mesoporous silica sample (a) and the immobilized complexes **1** (b), suggesting the retention of highly ordered structures even after the loading of the metal complex.

In the N_2 sorption isotherms for mesoporous host and the immobilized complexes, typical type IV isotherms with a steep rise due to capillary condensations, characteristic of mesoporous materials,[75,76] were seen. N_2 adsorption/desorption isotherms for mesoporous silica material and complex **1** immobilized on the silica are shown in Fig. 5. BET surface area and average pore diameter for the 2D-hexagonal mesoporous host (**HMS**) was 1438 m^2 g^{-1} and 2.8 nm, respectively. The BJH pore-size distribution suggested a very narrow range, centered at 2.8 nm for this 2D-hexagonal mesoporous material (inset of Fig. 5). Adsorption studies were also carried out for the complex immobilized samples. The surface area and pore diameters for immobilized samples **IC-1**, immobilized complex **2**·CH_3CN (**IC-2**), immobilized complex **3** (**IC-3**) and immobilized complex **4** (**IC-4**) were 1055 m^2 g^{-1} and 2.49 nm; 1025 m^2 g^{-1} and 2.47 nm; 1005 m^2 g^{-1} and 2.43 nm; 1010 m^2 g^{-1} and 2.44 nm, respectively. The surface areas for all the samples were found to be somewhat less than that of the **HMS** sample and also a decrease in the pore diameter could be observed. The decrease in pore diameter can be attributed to the metal centers adhered to the inner wall of the pores, which put forth a reducing effect on the pore size. Pore wall thickness is quite slim, which might help the catalytic sites to be located closer at the surface of the catalyst. HRTEM image of the as-synthesized sample is shown in the ESI† (Fig. S6) and it reveals hexagonal

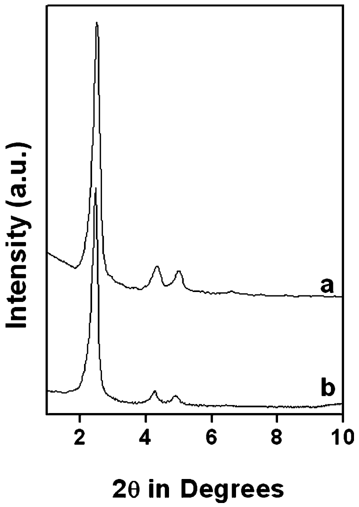

Fig. 4 Low angle X-ray diffraction patterns of (a) mesoporous silica and (b) immobilized complex **1** (**IC-1**) (representative case).

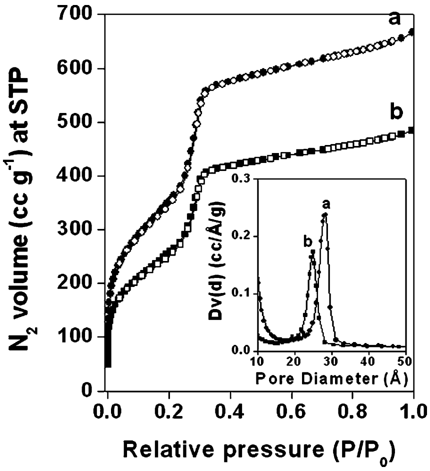

Fig. 5 N_2 adsorption/desorption isotherms for (a) mesoporous silica material and (b) complex **1** immobilized on the silica. Inset: Pore size distributions of (a) mesoporous silica material and (b) immobilized complex **1**.

Published on 19 September 2009. Downloaded by University of Michigan Library on 22/10/2014 13:10:09.

arrangement of the pores with different contrast than that of the pore walls. The average pore diameter for this sample agrees well with the N_2 sorption data. Electron diffraction pattern shown in the inset of this figure further suggested hexagonal arrangement of the pore channels.

Similarity in the UV-vis spectra suggests loading of the metal complex on the mesoporous materials (see later). Chemical analysis (atomic absorption spectroscopy, AAS) data further indicated 6.7, 7.1, 6.5 and 6.6 wt% of copper is present the mesoporous host for complexes **1**, **2**·CH_3CN, **3** and **4** respectively.

Heterogeneous catalysis

The epoxidation reactions of cyclohexene, styrene, α-methylstyrene and *trans*-stilbene were carried out heterogeneously with complexes **1–4** as the catalysts. In Table 7, results of the catalytic activities of four different Cu complexes immobilized over 2D-hexagonal mesoporous silica material are shown. Acetonitrile has been used as the solvent in all these liquid phase oxidation reactions. The major products for the partial oxidation of all four olefins are their respective epoxides. It is clear from the Table 7 that the selectivity of the epoxide for all the substrates is quite high. The conversion of the substrate enhances with time and after 24 h the conversion reaches its saturation. However, a few hours after the conversions reaching the respective maxima, epoxide selectivities go down considerably and their respective diol selectivity goes up. This could be attributed to the hydrolysis of the epoxides, which is quite common for the liquid phase partial oxidation of olefin over a heterogeneous catalyst[77,78] as water coming from the oxidant in the reaction mixture promotes the epoxide ring opening. In Table 7, turnover frequencies (TOFs) for different catalytic runs are also given. TOF for cyclohexene conversion is relatively more than that for styrene, α-methylstyrene and *trans*-stilbene. Among the immobilized catalysts used in this study, **IC-4** shows maximum reactivity in the conversion of cyclohexene and *trans*-stilbene with 90 and 77% yields respectively. **IC-2** is found to be the most effective catalyst for the epoxidation of styrene with 78% conversion. In the case α-methylstyrene **IC-3** is the most active catalyst with 76% conversion. As seen from the table, TOFs for the immobilized catalysts have been enhanced drastically *vis-à-vis* the metal complexes without any loss in epoxide selectivity. Cu–hydroperoxo species could be formed at the active sites in the presence of hydrogen peroxide as the oxidant (see later). Hydrophobic aromatic ligands attached to Cu centers in the immobilized catalyst could provide the affinity towards the olefinic substrates. This may facilitate the adsorption of the substrates near the vicinity of the active sites and their subsequent epoxidations. This could be responsible for high TOFs in these liquid phase partial oxidation reactions.

Table 7 Epoxidation of olefins over the immobilized Cu(II) complexes[a]

Substrate		IC-1	IC-2	IC-3	IC-4	IC-4[d]	Blank[e]
Cyclohexene	Conversion[b]	78	85	88	90	78	30
	Selectivity	90	87	92	87	90	26
	TOF[c]	12.0	13.3	17.0	12.0		
Styrene	Conversion[b]	75	78	73	67		
	Selectivity	91	88	85	90		
	TOF[c]	9.1	9.6	11.1	13.7		
α-Methylstyrene	Conversion[b]	68	73	76	70		
	Selectivity	85	82	88	85		
	TOF[c]	7.7	8.4	10.8	9.9		
trans-Stilbene	Conversion[b]	72	73	75	77		
	Selectivity	87	92	89	90		
	TOF[c]	5.0	5.2	6.6	6.8		

[a] Solvent: CH_3CN; temperature: 333 K; oxidant: hydrogen peroxide; catalyst: complexes immobilized on mesoporous silica. [b] Conversions were measured after 24 h of the reaction. [c] TOF: turnover frequency = moles of substrate converted per mole of Cu center per hour. [d] Re-used catalyst (**IC-4**) for fifth cycle under the same conditions. [e] Blank reaction without any catalyst, under identical experimental conditions.

We have examined whether the heterogeneous catalysts can be used further or not. For this purpose, one control experiment has been performed for cyclohexene (as a representative case) over immobilized catalyst to check the subsequent efficiency of catalytic cycles and also to check whether Cu leaches out from the catalyst. We have selected heterogeneous epoxidation of cyclohexene by **IC-4** as the representative case because it can be clearly seen in Table 7 that the maximum conversion of substrate can be achieved with this combination. The catalyst has been recovered by filtration, washed thoroughly with acetonitrile and then treated with 0.1 M HCl solution in ethanol for 8 h at 70 °C and finally dried at 100 °C for 2 h. The catalytic reaction has been performed following the same experimental procedure. The activity of the catalyst is decreased by a small amount in the subsequent cycles. It has been seen after repeating the catalytic cycles that the catalyst can be reused for at least five times without significant loss of activity (Table 7). In Fig. 6 we have plotted the catalytic activity in five consecutive cycles for the oxidation of cyclohexene over **IC-4**. As seen from this bar diagram, the catalytic activity decreases marginally in the successive cycles. However, epoxide selectivity remains almost the same in these repetitive reactions (Table 7). Any Cu species present in the reaction mixture could catalyze the olefin epoxidation. Hence, atomic absorption spectroscopy has been used to determine the amount of copper leached out into the reaction mixture and it was found that there is almost no Cu leaching into the liquid phase from these immobilized catalysts. A blank reaction in the absence of any immobilized catalyst under identical experimental conditions has

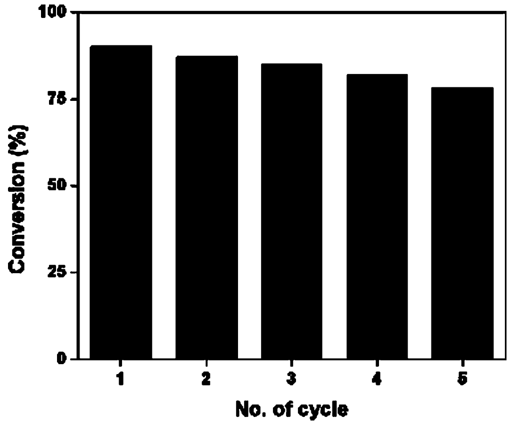

Fig. 6 Catalytic activity of complex **4** immobilized on mesoporous silica for epoxidation of cyclohexene. The activity of the catalyst decreases with increasing number of catalytic cycles.

This journal is © The Royal Society of Chemistry 2009

Published on 19 September 2009. Downloaded by University of Michigan Library on 22/10/2014 13:10:09.

Table 8 Epoxidation[a] of olefins over Cu(II) complexes

Substrate		Complex **1**	Complex **2**	Complex **3**	Complex **4**	Blank 1[d]	Blank 2[e]
Cyclohexene	Conversion[b]	88	90	92	95	30	42
	Selectivity	91	89	92	86	26	50
	TOF[c]	5.6	5.7	5.8	6.0		
Styrene	Conversion[b]	85	88	83	81		
	Selectivity	90	89	88	92		
	TOF[c]	4.2	4.4	4.1	4.0		
α-methylstyrene	Conversion[b]	78	83	84	83		
	Selectivity	87	85	86	87		
	TOF[c]	3.6	3.8	3.9	3.8		
trans-stilbene	Conversion[b]	76	78	75	76		
	Selectivity	88	93	89	92		
	TOF[c]	2.2	2.3	2.2	2.2		

[a] Solvent: CH_3CN; temperature: 298 K; oxidant: hydrogen peroxide; catalyst: 0.01 mmol complexes. [b] Conversions were measured after 24 h of the reaction. [c] TOF: turnover frequency = moles of substrate converted per mole of Cu center per hour. [d] Blank reaction without any catalyst, under the same experimental conditions. [e] Blank reaction in the presence of $CuCl_2$, under same experimental conditions.

also been carried out (Table 7). The result shows very poor conversion and epoxide selectivity in this case, thereby confirming the catalytic role of the Cu complex and the immobilized catalyst in these epoxidation reactions. The reactivity of the immobilized catalysts can be compared with other transition metal complexes heterogenized on silica. The present systems are less or comparable in catalytic activities with Mn complexes,[79–81] Mo complexes,[82,83] Ru complexes,[84] and V complexes.[85] The catalytic results obtained by our previous immobilized Ni[56] or Cu[57]–Schiff-base complexes or Cu(I) complexes[86] are comparable with the present systems.

Homogenous catalysis

The homogeneous catalysis for the epoxidation of the olefins was carried out using hydrogen peroxide as the oxidant at room temperature. The results of the conversion of cyclohexene, styrene, α-methylstyrene and *trans*-stilbene are shown in Table 8. It can be clearly seen from the table that all substrates are converted in good yield. Respective epoxides are the major products for the every reaction. Among the substrates, the conversion of cyclohexene is highest with 95% yield in the presence of complex **4** as the catalyst. Selectivity of cyclohexane epoxide in the presence of complex **4** is 86%. However, the conversion of *trans*-stilbene to its epoxide is lowest for all the catalysts. The highest conversion of styrene is 88% in presence of complex **2**·CH_3CN. Complex **3** is the most active catalyst for the epoxidation of α-methylstyrene with 84% conversion and the selectivity for epoxide is 86%. It has been observed that during the catalytic reaction, the yield of the reaction increases with time and after a certain time it seems that the conversion reaches its saturation. A blank reaction is carried out without any catalyst under same experimental conditions. The result for that reaction shows a remarkable decrease in the conversion of the substrate as well as the epoxide selectivity with no metal complex. Another blank reaction is carried out in the presence of copper(II) chloride under the same experimental conditions. The results show an improvement of the conversion and epoxide selectivity in comparison to the conversion of cyclohexene with no catalyst or metal salt. But the conversion is notably lower than the conversion of cyclohexene in the presence of the catalyst. It is evident that the presence of N,O-donor ligands is quite relevant. Conversion and product selectivity for the catalyzed reactions have been improved a lot for the homogeneous and heterogeneous catalytic reactions, suggesting the catalytic role played by the Cu(II) centers in these partial oxidation reactions. The catalytic activities of the complexes in a homogeneous medium are lower or comparable in conversion of the substrate and epoxide selectivity in comparison with W(VI) complex or Mo catalyst,[87–89] Mn catalyst,[90–92] and Fe–porphyrin complexes,[93,94] but these are more active catalysts in comparison to previously reported Cu complexes.[95–97]

Spectral studies

UV-vis spectra for all the complexes were recorded in both solution phase (in acetonitrile) and solid phase (immobilized catalyst) at room temperature. All the complexes behave in a similar way. They showed peaks in the range of 253–263 nm. These peaks may be attributed to the $\pi \rightarrow \pi^*$ transition. Their absorption peaks in the range of 381 to 388 nm may be due a charge transfer transition. They showed a relatively broad band at around 670 nm, which may be assigned as the d–d transition. On the other hand, the immobilized complexes showed a broad absorption ranging from 360–430 nm, with maxima at *ca.* 385 nm. This similarity of the absorbance bands in solution and solid phase confirms that the complexes are also present in solid silica material, *i.e.* the loading of the complexes into the mesoporous silica.

The electrospray ionisation mass spectra of all the complexes were recorded in acetonitrile at room temperature. The complexes **1**, **2**·CH_3CN, **3** and **4** show peaks at m/z 1154.36, 1130.18, 1402.17 and 1402.17 respectively. The peaks can be assigned to $[Cu_4(O)(\mathbf{L}^n)_2(CH_3COO)_3]^+$ species where n = 1, 2, 3 and 4 for complexes **1**, **2**·CH_3CN, **3** and **4**, respectively. It is clearly evident from the above data that each complex loses one acetate ion in solution (complex **2**·CH_3CN also loses acetonitrile). Thus this monocationic species may be the catalytically active species in solution.

To check the effect of hydrogen peroxide, we recorded the UV-vis spectra of complexes in the presence of H_2O_2 in acetonitrile. The

Published on 19 September 2009. Downloaded by University of Michigan Library on 22/10/2014 13:10:09.

effect of H_2O_2 on the UV-vis spectra of complex **1** is shown in Fig. 7 as the representative case. It has been observed that an intense peak at around 400 nm with a shoulder in the range of 415–440 nm appears. This may be due to the existence of Cu–hydroperoxo or Cu–peroxo species.[18,57] UV-vis spectra of complexes immobilized on mesoporous silica in the presence of hydrogen peroxide were also recorded and show similar absorption bands to those of just the complex in the presence of H_2O_2. That means that Cu–hydroperoxo or Cu–peroxo species is also generated during the heterogeneous catalysis. This may be the active species for the conversion of the olefins.

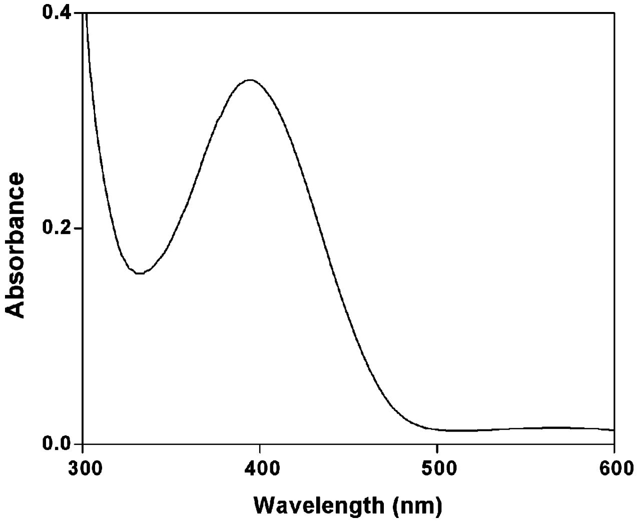

Fig. 7 UV-vis spectrum of complex **1** in presence of hydrogen peroxide in acetonitrile at room temperature.

The transfer of the oxygen atom from the peroxo species to the olefins may be stepwise or concerted. During the catalytic conversion, the procedure involves first coordination of alkene to the metal center forming a metalloperoxocyclic intermediate.[98] For the initial coordination of alkene, the metal center needs a vacant coordination site. The metal atoms in all of the complexes are five coordinated having labile sites like Cu–μ_4-oxo or Cu–acetate. In solution, it has been seen by ESI mass spectroscopy that each tetranuclear Cu(II) complex loses one acetate ion. So there is the necessary vacant site for ligation. Then epoxide along with the catalyst is formed by the cycloreversion of that intermediate. Khaliullin *et al.* have shown that in vanadium complexes with pyrazine-2-carboxylic acid (an N,O-donor ligand) the O atom of the ligand takes up a proton rather than a nitrogen atom.[99] Hence it may be assumed that the proton transfer from the OH moiety to one oxygen atom of the ligand and the breakage of the M–O bond is the step preceding the reaction with alkene and formation of the intermediate. One cannot rule out that the epoxidation may be considered as a concerted one step reaction where a direct attack of the substrate on the peroxo species occurs.[100]

Conclusion

We have been able to synthesize and characterize four tetranuclear copper(II) complexes with N_2O-donor Schiff-base ligands by single crystal X-ray diffraction analyses. The structural analyses show that all of them are μ_4-oxo-bridged tetranuclear monomeric compounds. Magnetic properties of the complexes were measured in the temperature range 5–300 K and the study revealed an exceptionally strong antiferromagnetic coupling among the copper atoms in the (Cu_4–O) cluster. These have been employed as the active catalysts for the epoxidation of olefins using hydrogen peroxide as the oxidant. The catalytic reactions were carried out homogeneously as well as heterogeneously. Heterogeneous catalytic reactions were carried out over the metal complexes immobilized on 2D hexagonal mesoporous silica as the catalyst. The results reveal that the conversion of the olefin is quite high and epoxides were produced with high selectivity. Conversion of the substrate in homogeneous catalysis is more than that in heterogeneous catalysis. But in the case of heterogeneous catalysis, it has been evident that the catalyst can be reused for at least five times without appreciable loss in activity after recovering it by simple filtration. By comparing the results of catalysis we can conclude that the heterogeneous catalyst is more effective than the homogeneous one. The application of copper(II) complexes as catalysts for the epoxidation of alkenes in either homogeneous medium or heterogeneous medium has rarely been reported to date.

Acknowledgements

PR wishes to thank Jadavpur University for providing a JU research grant. MN acknowledges the CSIR, New Delhi, for a Junior Research Fellowship. AB wishes to thank the Department of Science and Technology, New Delhi, for providing a Ramanna Fellowship and research grants. This work was partly funded by the Nanoscience and Technology Initiative of DST, Government of India.

References

1 M. Zhao, C. Zhong, C. Stern, A. G. M. Barrett and B. M. Hoffman, *J. Am. Chem. Soc.*, 2005, **127**, 9769–9775.
2 S. Triki, C. J. Gomez-Garcia, E. Ruiz and J. Sala-Pala, *Inorg. Chem.*, 2005, **44**, 5501–5508.
3 J. Yoon, L. M. Mirica, T. D. P. Stack and E. I. Solomon, *J. Am. Chem. Soc.*, 2004, **126**, 12586–12595.
4 Y. Song, C. Massera, O. Roubeau, P. Gamez, A. M. M. Lanfredi and J. Reedijk, *Inorg. Chem.*, 2004, **43**, 6842–6847.
5 K. S. Banu, T. Chattopadhyay, A. Banerjee, S. Bhattacharya, E. Suresh, M. Nethaji, E. Zangrando and D. Das, *Inorg. Chem.*, 2008, **47**, 7083–7093.
6 N. A. Rey, A. Neves, A. J. Bortoluzzi, C. T. Pich and H. Terenzi, *Inorg. Chem.*, 2007, **46**, 348–350.
7 M. E. Bluhm, M. Ciesielski, H. Görls, O. Walter and M. Döring, *Inorg. Chem.*, 2003, **42**, 8878–8885.
8 K. Dhara, S. Karan, J. Ratha, P. Roy, G. Chandra, M. Manassero, B. Mallik and P. Banerjee, *Chem.–Asian J.*, 2007, **2**, 1091–1100.
9 K. Dhara, P. Roy, J. Ratha, M. Manassero and P. Banerjee, *Polyhedron*, 2007, **26**, 4509–4517.
10 R. Robson, *Aust. J. Chem.*, 1970, **23**, 2217–2224.
11 R. Robson, *Inorg. Nucl. Chem. Lett.*, 1970, **6**, 125–128.
12 H. Okawa, H. Furutachi and D. E. Fenton, *Coord. Chem. Rev.*, 1998, **174**, 51–75, and references therein.
13 S. Torelli, C. Belle, I. Gautier Luneau, J. L. Pierre, E. S. Aman, J. M. Latour, L. Le Pape and D. Luneau, *Inorg. Chem.*, 2000, **39**, 3526–3536.
14 S. Mukherjee, T. Weyhermüller, E. Bothe, K. Wieghardt and P. Chaudhuri, *Eur. J. Inorg. Chem.*, 2003, 863–875.
15 P. Roy, K. Dhara, M. Manassero and P. Banrejee, *Inorg. Chim. Acta*, 2009, **362**, 2927–2932.
16 P. Roy, M. Manassero, K. Dhara and P. Banrejee, P., *Polyhedron*, 2009, **28**, 1133–1137.

This journal is © The Royal Society of Chemistry 2009

View Article Online

Published on 19 September 2009. Downloaded by University of Michigan Library on 22/10/2014 13:10:09.

17 C. A. Reed and R. D. Orosz, Spin Coupling Concepts in Bioinorganic Chemistry, in *Research Frontiers in Magnetochemistry*, ed. C. J. O'Connor, World Scientific, Singapore, 1993, p. 351.

18 J. Reim, R. Werner, W. Haase and B. Krebs, *Chem.–Eur. J.*, 1998, **4**, 289–298.

19 P. Roy, K. Dhara, M. Manassero and P. Banrejee, *Eur. J. Inorg. Chem.*, 2008, 4404–4412.

20 J. Reim, K. Griesar, W. Haase and B. Krebs, *J. Chem. Soc., Dalton Trans.*, 1995, 2649–2656.

21 Y. S. You, J. H. Yoon, H. C. Kim and C. S. Hong, *Chem. Commun.*, 2005, 4116–4118.

22 M. Du, Y. M. Guo, S. T. Chen, X. H. Bu, S. R. Batten, J. Ribas and S. Kitagawa, *Inorg. Chem.*, 2004, **43**, 1287–1293.

23 M. Bera, W. Tak Wong, G. Aromi, J. Ribas and D. Ray, *Inorg. Chem.*, 2004, **43**, 4787–4789.

24 A. R Paital, P. K. Nanda, S. Das, G. Aromi and D. Ray, *Inorg. Chem.*, 2006, **45**, 505–507.

25 L. Canali and D. C. Sherrington, *Chem. Soc. Rev.*, 1999, **28**, 85–93.

26 K. C. Gupta and A. K. Sutar, *Coord. Chem. Rev.*, 2008, **252**, 1420–1450.

27 K.A. Jorgensen, *Chem. Rev.*, 1989, **89**, 431–458.

28 T. Mukaiyama and T. Yamada, *Bull. Chem. Soc. Jpn.*, 1995, **68**, 17–35.

29 A. K. Rahiman, K. S. Bharathi, S. Sreedaran and V. Narayanan, *Catal. Lett.*, 2009, **127**, 175–182.

30 A. K. Rahiman, K. Rajesh, K. S. Bharathi, S. Sreedaran and V. Narayanan, *Inorg. Chim. Acta*, 2009, **362**, 1491–1500.

31 M. Moghadam, V. Mirkhani, S. Tangestaninejad, I. Mohammdpoor-Baltork and H. Kargar, *J. Mol. Catal. A: Chem.*, 2008, **288**, 116–124.

32 S.-H. Cho, T. Gadzikwa, M. Afshari, S. T. Nguyen and J. T. Hupp, *Eur. J. Inorg. Chem.*, 2007, 4863–4867.

33 L. Gómez, I. Garcia-Bosch, A. Company, X. Sala, X. Fontrodona, X. Ribas and M. Costas, *Dalton Trans.*, 2007, 5539–5545.

34 N. M. F. Carvalho, O. A. C. Antunes and A. Horn, Jr., *Dalton Trans.*, 2007, 1023–1027.

35 M. Pratt, J. B. Harper and S. B. Colbran, *Dalton Trans.*, 2007, 2746–2748.

36 J. Zhao, K. R. Jain, E. Herdtweck and F. E. Kühn, *Dalton Trans.*, 2007, 5567–5571.

37 S.-H. Cho, B. Ma, S. T. Nguyen, J. T. Hupp and T. E. Albrecht-Schmitt, *Chem. Commun.*, 2006, 2563–2565.

38 Y. Watanabe, A. Namba, N. Umezawa, M. Kawahata, K. Yamaguchi and T. Higuchi, *Chem. Commun.*, 2006, 4958–4962.

39 R. I. Kureshy, N. H. Khan, S. H. Abdi, S. t. Patel, P. Iyer, E. Suresh and P. Dastidar, *J. Mol. Catal. A: Chem.*, 2000, **160**, 217–227.

40 H. Yoon, T. R. Wagner, K. J. O'Connor and C. J. Burrows, *J. Am. Chem. Soc.*, 1990, **112**, 4568–4570.

41 R. Noyori, M. Aoki and K. Sato, *Chem. Commun.*, 2003, 1977–1986.

42 M. Tada and Y. Iwasawa, *Coord. Chem. Rev.*, 2007, **251**, 2702–2716.

43 F. Biginame, A. Corradini, C. Quarantelli and G. Sartori, *J. Catal.*, 2007, **250**, 222–230.

44 M. R. Maurya, S. J. J. Titinchi and S. Chand, *J. Mol. Catal. A: Chem.*, 2003, **201**, 119–130.

45 S. Mukherjee, S. Samanta, A. Bhaumik and B. C. Ray, *Appl. Catal., B*, 2006, **68**, 12–20.

46 Y. Liu, K. Murata, M. Inaba and N. Mimura, *Catal. Commun.*, 2003, **4**, 281–285.

47 H. U. Blaser, B. Pugin and F. Spinder, *J. Mol. Catal. A: Chem.*, 2005, **231**, 1–20.

48 M. S. Saraiva, N. L. D. Filho, C. D. Nunes, P. D. Vaz, T. G. Nunes and M. J. Calhorda, *Microporous Mesoporous Mater.*, 2009, **117**, 670–677.

49 S. M. Coman, M. Florea, V. I. Parvulescu, V. David, A. Medvedovici, D. De Vos, P. A. Jacobs, G. Poncelet and P. Grange, *J. Catal.*, 2007, **249**, 359–369.

50 P. McMorn and G. J. Hutching, *Chem. Soc. Rev.*, 2004, **33**, 108–122.

51 A. R. Silva, V. Budarin, J. H. Clark, C. Freire and B. de Castro, *Carbon*, 2007, **45**, 1951–1964.

52 A. R. Silva, M. Martins, M. M. A. Freitas, J. L. Figueiredo, C. Freire and B. de Castro, *Eur. J. Inorg. Chem.*, 2004, 2027–2035.

53 I. Kuzniarska-Biernacka, A. R. Silva, R. Ferreira, A. P. de Carvalho, J. Pires, M. B. de Carvalho, C. Freire and B. de Castro, *New J. Chem.*, 2004, **28**, 853–858.

54 R. Ferreira, M. Silva, C. Freire, B. de Castro and J. L. Figueiredo, *Microporous Mesoporous Mater.*, 2000, **38**, 391–401.

55 J. J. Cowell, A. K. Santra, R. Lindsay, R. M. Lambert, A. Baraldi and A. Goldoni, *Surf. Sci.*, 1999, **437**, 1–8.

56 J. Chakraborty, M. Nandi, H. Mayer-Figge, W. S. Sheldrick, L. Sorace, A. Bhaumik and P. Banerjee, *Eur. J. Inorg. Chem.*, 2007, 5033–5044.

57 P. Roy, K. Dhara, M. Manassero and P. Banerjee, *Inorg. Chem. Commun.*, 2008, **11**, 265–269.

58 R. R. Gagne, C. L. Spiro, T. J. Smith, C. A. Hamann, W. R. Thies and A. K. Schiemke, *J. Am. Chem. Soc.*, 1981, **103**, 4073–4081.

59 D. D. Perrin, W. L. F. Armarego and D. R. Perrin, *Purification of Laboratory Chemicals*, Pergamon Press, Oxford, U.K., 1980.

60 J. J. Grzybowski and F. L. Urbach, *Inorg. Chem.*, 1980, **19**, 2604–2608.

61 P. Roy, K. Dhara, M. Manassero, J. Ratha and P. Banerjee, *Inorg. Chem.*, 2007, **46**, 6405–6412.

62 *SAINT Reference manual*, Siemens Energy and Automation, Madison, W1, 1994–1996.

63 G. M. Sheldrick, *SADABS, Empirical Absorption Correction Program*, University of Gottingen, Germany, 1997.

64 B.A. Frenz, *Comput. Phys.*, 1988, **2**, 42.

65 *Crystallographic Computing 5*, Oxford University Press, Oxford, U.K., 1991, ch. 11, pp. 126.

66 G. M. Sheldrick, *SHELXS 86. Program for the solution of crystal structures*, University of Gottingen, Germany, 1985.

67 R. Karmakar, C. Roy Choudhury, D. L. Hughes and S. Mitra, *Inorg. Chim. Acta*, 2007, **360**, 2631–2637.

68 P. Roy, *J. Coord. Chem.*, 2009, **62**, 2003–2011.

69 J. T. Guy, Jr., J. C. Cooper, R. D. Gilardi and J. L. Flippen-Anderson, *Inorg. Chem.*, 1988, **27**, 635–638.

70 A.W. Addison, T. N. Rao, J. Reedijk, J. Vanrijn and G. C. Verschoor, *J. Chem. Soc., Dalton Trans.*, 1984, 1349–1356.

71 J. H. Van Vleck, *Nobel Lectures, Physics 1971–1980*, World Scientific Publishing, Singapore, 1992, pp. 353–369.

72 S. Teipelf, K. Griesar, W. Haase and B. Krebs, *Inorg. Chem.*, 1994, **33**, 456–464.

73 B. Bleaney and K.D. Bowers, *Proc. R. Soc. London, Ser. A*, 1952, **214**, 451–465.

74 M. Riccò, T. Shiroka, S. Carretta, F. Bolzoni, C. Femoni, M. C. Iapalucci and G. Longoni, *Chem.–Eur. J.*, 2005, **11**, 2856.

75 C. T. Kresge, M. E. Leonowicz, W. J. Roth, J. C. Vartuli and J. S. Beck, *Nature*, 1992, **359**, 710–712.

76 D. Chandra, B. K. Jena, C. R. Raj and A. Bhaumik, *Chem. Mater.*, 2007, **19**, 6290–6296.

77 A. Bhaumik and T. Tatsumi, *Chem. Commun.*, 1998, 463–464.

78 A. Bhaumik and T. Tatsumi, *J. Catal.*, 1999, **182**, 349–356.

79 H. Zhang, S. Xiang and C. Li, *Chem. Commun.*, 2005, 1209–1211.

80 A. S. Amarasekara, I. McNeal, J. Murillo, D. Green and A. Jennings, *Catal. Commun.*, 2008, **9**, 2437–2440.

81 K. Yu, Z. Gu, R. Ji, L.-L. Lou and S. Liu, *Tetrahedron*, 2009, **65**, 305–311.

82 S. Tangestaninejad, M. Moghadam, V. Mirkhani, I. Mohammadpoor-Baltork and K. Ghani, *Inorg. Chem. Commun.*, 2008, **11**, 270–274.

83 B. Monteiro, S. S. Balula, S. Gago, C. Grosso, S. Figueiredo, A. D. Lopes, A. A. Valente, M. Pillinger, J. P. Lourenço and I. S. Gonçalves, *J. Mol. Catal. A: Chem.*, 2009, **297**, 110–117.

84 Okumura, H. Takagi, Y. Funahashi, T. Ozawa, Y. Fukushima, K. Jitsukawa and H. Masuda, *Chem. Lett.*, 2007, **36**, 122–123.

85 R. Sen, R. Bera, A. Bhattacharjee, P. Gütlich, S. Ghosh, A. K. Mukherjee and S. Koner, *Langmuir*, 2008, **24**, 5970–5975.

86 M. M. Díaz-Requejo, T. R. Belderraín and P. J. Pérez, *Chem. Commun.*, 2000, 1853–1854.

87 S. K. Maiti, S. Dinda, N. Gharah and R. Bhattacharyya, *New J. Chem.*, 2006, **30**, 479–489.

88 C. Venturello, R. D'Aloisio, J. C. Bart and M. Ricci, *J. Mol. Catal.*, 1985, **32**, 107–110.

89 K. Sato, M. Aoki, M. Ogowa, T. Hasimoto and R. Noyori, *J. Org. Chem.*, 1996, **61**, 8310–8311.

90 S. Banfi, F. Legramandi, F. Montanari, G. Pozzi and S. Quici, *J. Chem. Soc., Chem. Commun.*, 1991, 1285–1287.

91 P. L. Anelli, L. Banfi, F. Legramandi, F. Montanari, G. Pozzi and S. Quici, *J. Chem. Soc., Perkin Trans. 1*, 1993, 1345–1357.

92 R. I. Kureshy, N.-ul. H. Khan, S.H.R. Abdi, I. Ahmad, S. Singh and R.V. Jasra, *J. Catal.*, 2004, **221**, 234–240.

Published on 19 September 2009. Downloaded by University of Michigan Library on 22/10/2014 13:10:09.

93 J. F. Bartoli, P. Battioni, W. R. De Foor and D. J. Mansuy, *J. Chem. Soc., Chem. Commun.*, 1994, 23–24.
94 W. Nam, S. W. Jin, M. H. Lim, J. Y. Ryu and C. Kim, *Inorg. Chem.*, 2002, **41**, 3647–3652.
95 G. Das, R. Shukla, S. Mandal, R. Singh, P. K. Bharadwaj, J. v. Hall and K.H. Whitmire, *Inorg. Chem.*, 1997, **36**, 323–329.
96 S. Zolezzi, E. Spodine and A. Decinti, *Polyhedron*, 2003, **22**, 1653–1658.
97 E. H. Kim, D. I. Kim, H. S. Lee, H. G. Na, J. C. Byun, J. H. Choi and Y. C. Park, *Polyhedron*, 2007, **26**, 85–92.
98 H. Mimoun, I. Seree de Roch and L. Sajus, *Tetrahedron*, 1970, **26**, 37–50.
99 R. Z. Khaliullin, A. T. Bell and M. Head-Gordon, *J. Phys. Chem. B*, 2005, **109**, 17984–17992.
100 K. B. Sharpless, J. M. Townsend and D. R. Williams, *J. Am. Chem. Soc.*, 1972, **94**, 295–296.

This journal is © The Royal Society of Chemistry 2009